Transactions on Automatic Control, Vol. AC-21, No. 6, 1976, pp. 866–869.

[8]Rozonoer, L. I., "L.S. Pontryagin Maximum Principle in Optimal System Theory," *Optimal and Self-Optimizing Control,* edited by R. Oldenburger, MIT Press, Cambridge, MA, 1966, pp. 210–257.

[9]Keller, H. B., *Numerical Solution of Two-Point Boundary Value Problems,* Regional Conference Series in Applied Mathematics, No. 24, Society of Industrial and Applied Mechanics, Philadelphia, PA, 1976.

[10]Ascher, U. M., Mattheij, R. M. M., and Russell, R. D., *Numerical Solution of Boundary Value Problems for Ordinary Differential Equations,* Prentice-Hall, Englewood Cliffs, NJ, 1988.

[11]Ascher, U. M., and Russell, R. D., "Reformulation of Boundary Value Problems into 'Standard Form,'" *SIAM Review,* Vol. 23, 1981, pp. 238–254.

[12]Lentini, M., and Pereyra, V., "PASVA4: An O.D.E. Boundary Solver for Problems with Discontinuous Interfaces and Algebraic Parameters," *Mathematical Application in Computing,* Vol. 2, No. 2, 1983, pp. 103–118.

[13]Pereyra, V., "Deferred Corrections Software and Its Application to Seismic Ray Tracing," *Computing,* Suppl. 5, 1984, pp. 211–226.

[14]Henrici, P., *Discrete Variable Methods in Ordinary Differential Equations,* Wiley, New York, 1962.

[15]Osborne, M. R., "On Shooting Methods for Boundary Value Problems," *Journal of Mathematical Analysis and Applications,* Vol. 27, No. 2, 1969, pp. 417–433.

[16]Deuflhard, P., and Bader, G., "Numerical Techniques Revisited," *Numerical Treatment of Inverse Problems in Differential and Integral Equations,* edited by P. Deuflhard and E. Hairer, Birkhauser, Boston, MA, 1983, pp. 74–122.

Compensating Sampling Errors in Stabilizing Helmet-Mounted Displays Using Auxiliary Acceleration Measurements

S. Merhav* and M. Velger†
Technion—Israel Institute of Technology, Haifa 32000, Israel

Introduction

THE visual acuity in helmet-mounted displays (HMD) under conditions of aircraft vibrations may be imparied by uncontrollable vibratory relative motion between the viewer's eye point-of-regard and the display. This vibratory motion often causes image blurring because the HMD vibrates with the pilot's head while his eyes are stabilized inertially by the vertibulo-ocular reflex.[1] To retain visual acuity, image stabilization on the HMD is needed.

Previous studies of Wells and Griffin[2,3] have shown the potential benefits of image stabilization in HMDs for retaining visual acuity under the conditions of whole-body vibrations. In their studies, the stabilization was performed by utilizing the double integrated head rotational acceleration signal, derived from at least one pair of helmet-mounted accelermeters, to shift the image on the display. This method, however, performed poorly when large-amplitude head rotations were executed.

An alternative method, which makes use of adaptive filtering to estimate the head motion due to the platform accelerations and uses this estimate to shift the image on the display, was devised.[4,5] This estimate is based on the readings of the helmet position and orientation measurement device. Such a device, whether magnetic or electro-optic, typically has a sampling rate of 30–60 Hz, which is dictated by computation time, sensor response time, and noise.[6] Futhermore, signal transmission and display computation time further reduce the effective rate. Head motion measurement devices with substantially higher rates are presently unavailable.

Since the desired image stabilization is in the frequency range of 3–8 Hz, the delay due to the sampling rate introduces a large phase shift, resulting in a significant stabilization error. This can be demonstrated by the following example. Denote θ as the true head orientation; thus, the delayed measurement would be $\theta\epsilon^{-\tau s}$ and the relative error can be expressed by

$$\epsilon = (\theta - \theta e^{-\tau s})/\theta = 1 - e^{-\tau s} = 1 - e^{-j\omega\tau} = 1 - \cos\omega\tau + j\sin\omega\tau \tag{1}$$

The absolute value of ϵ is

$$|\epsilon| = \left[(1-\cos\omega\tau)^2 + \sin^2\omega\tau\right]^{1/2} = \sqrt{2}(1-\cos\omega\tau)^{1/2} \tag{2}$$

For example, with $f = 5$ Hz and $\tau = 30$ ms, $|\epsilon| = 0.91$, i.e., 91% error. To reduce this error to an acceptable level of 10%, the sampling rate must be increased to about 300 Hz.

A method that overcomes this obstacle, based on complementary filtering, is described. It combines measurements of the head position and orientation system with measurements of the angular accelerations of the head, so as to reduce the phase shift in the head orientation measurements. Moreover, the complementary filter, if implemented either as an analog circuit, or digitally at much higher frequencies, substantially improves the resolution of the output signal.

Complementary Filter

A block diagram of the complementary filter is shown in Fig. 1. The two inputs to the filter are the head orientation vector $\boldsymbol{\Theta}$ and the head angular acceleration vector $\ddot{\boldsymbol{\Theta}}$. For brevity, only one component of each vector will be addressed in the sequel, i.e., θ and $\ddot{\theta}$, respectively. The orientation signal θ is obtained from the measurement system as a digital stream with a frequency of 30 Hz. As a result of the computations in the measurement system, this signal is delayed by T s and is constant for the duration of the sampling interval. The acceleration is measured at a much higher sampling rate and can be considered as a continuous signal. Referring to Fig. 1, the equation of the complementary filter is

$$\left\{\left[(1-e^{-Ts}/Ts)e^{-Ts}\theta - \hat{\theta}\right]\frac{a_0}{s} + s^2\theta + b + \left[(1-e^{-Ts}/Ts)e^{-Ts}\theta - \hat{\theta}\right]a_1\right\}\frac{1}{s} + \left[(1-e^{-Ts}/Ts)e^{-Ts}\theta - \hat{\theta}\right] \times a_2 = s\hat{\theta} \tag{3}$$

The output of the filter is the estimated head orientation, and accordingly is

$$\hat{\theta} = \frac{s^3 + a_2\eta s^2 + a_1\eta s + a_0\eta}{s^3 + a_2 s^2 + a_1 s + a_0}\theta + \frac{s}{s^3 + a_2 s^2 + a_1 s + a_0}b \tag{4}$$

where

$$\eta = \left[(1-e^{-Ts})/Ts\right]e^{-Ts}$$

and b is the bias of the accelerometer or noise. From Eq. (4) it is apparent that at high frequencies $\hat{\theta}\to\theta$. At low frequencies $\eta\to 1$, so that again $\hat{\theta}\to\theta$. The same argument holds for high sampling rates when $T\to 0$ again, $\eta\to 1$, and $\hat{\theta}\to\theta$. Also, from Eq. (4) it is clear that both the low- and high-frequency accel-

Received Feb. 1, 1990; revision received April 11, 1990.

*Professor, Department of Aerospace Engineering; also, Head, Flight Control Laboratory. Member AIAA.

†Consultant; also, Head, Control Systems Section, ELOP, Electro-Optics Ind., Rehovot, 76111, Israel. Member AIAA.

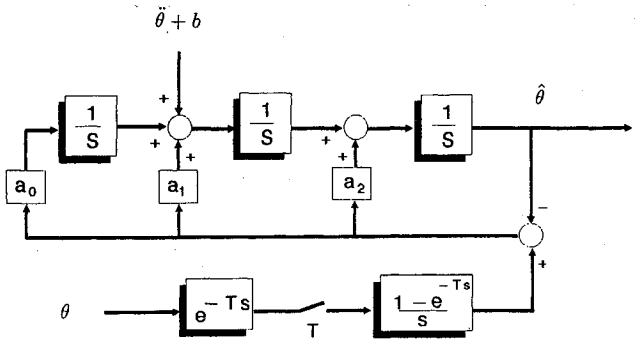

Fig. 1 Block diagram of complementary filter.

erometer noise is attenuated by the filter. It should be borne in mind that bias and gravity components are small because the accelerometer pair is arranged differentially.

As noted in Ref. 7, the complementary filter is actually a steady-state Kalman filter, with a_2, a_1, and a_0 determining the filter gains. Their values can be chosen to shape the filter frequency response, as shown in Fig. 2, which shows that the filter has unity gain response at both low and high frequencies. Also, for the chosen gains, the output of the filter is attenuated only slightly (less than 1 dB) in the intermediate frequencies. Similarly, the phase shift of the filter is zero at both low and high frequencies, and again there is only a small phase shift in the intermediate frequencies. Furthermore, in the frequencies of interest, i.e., 4–6 Hz, there is a slight phase lead that can compensate for further time delays due to display computations.

Simulation of the Complementary Filter

A simulation of the performance of the complementary filter was performed. A sinusoidal motion with a frequency of 5 Hz and an amplitude of 15 mrad for the head vibration was assumed. Such a motion is typical for whole-body vibration of $0.1g$. The filter parameters were $a_2=4.4$, $a_1=5.2$, and $a_0=3$. These parameters correspond to a second-order filter with $\omega_n=1$ rad/s and a damping ratio of $\zeta=0.7$, cascaded with a 3-rad/s first-order filter. This choice of the gains of the filter is a tradeoff between a good response to the initial condition mismatch of the integrators of the filter and assuring a small phase shift in the frequencies of interest. The noise of the orientation measurement system was assumed to be a white noise with $\sigma=0.1$ deg. The accelerometer noise data were taken for the Endevco model 7290-10 and were $0.003g$ rms up to 200 Hz. The threshold of $0.0005g$ of this accelerometer was also included in the simulations. These values were converted

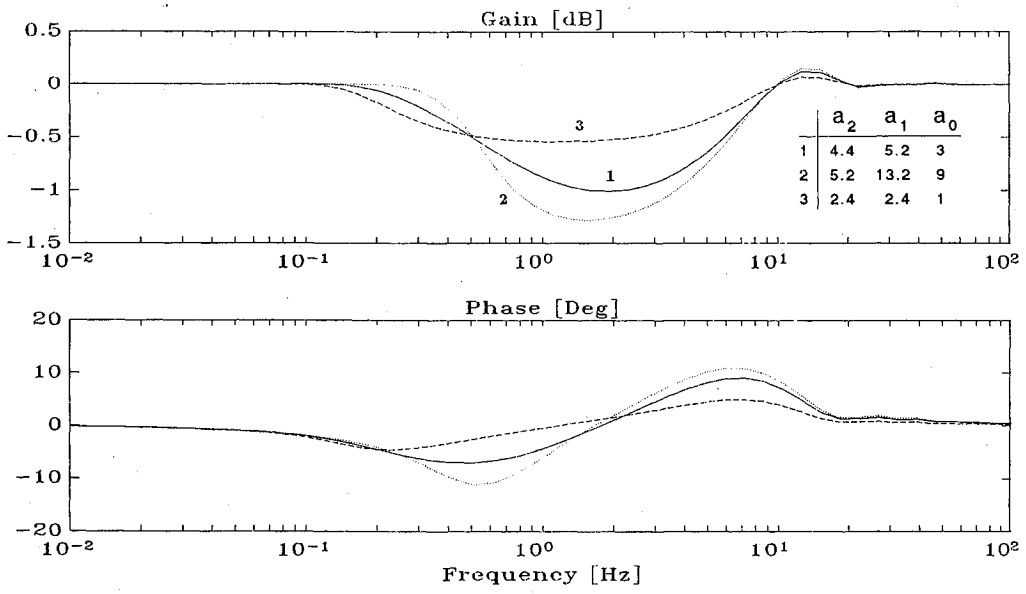

Fig. 2 Frequency response of complementary filter.

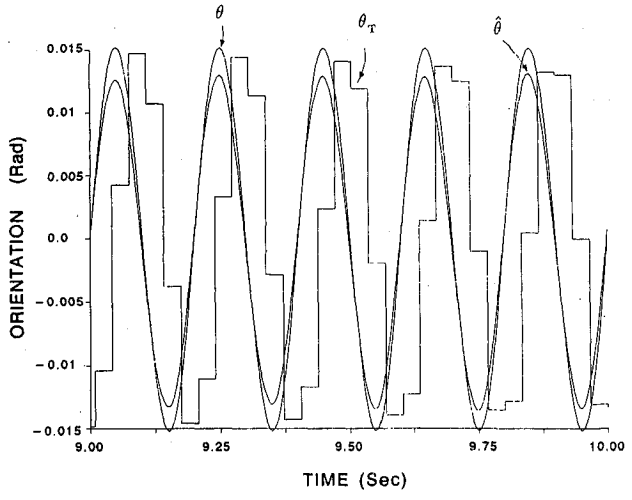

Fig. 3 Steady-state response of complementary filter. Shown are true head motion θ, estimated head motion $\hat{\theta}$, and delayed and sampled head motion θ_T as obtained from the HMD measurement system.

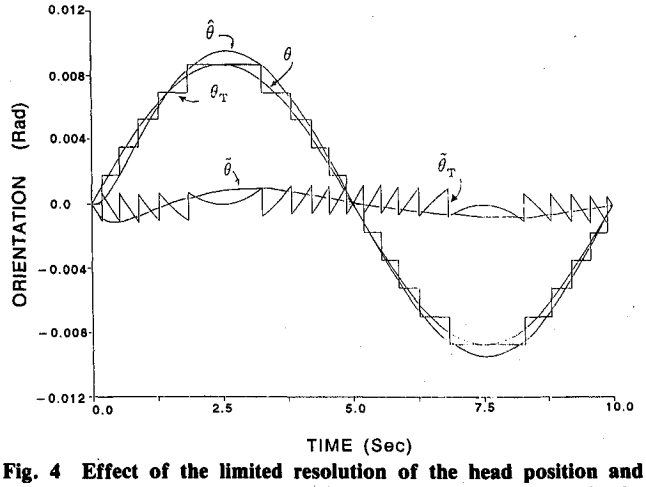

Fig. 4 Effect of the limited resolution of the head position and orientation measurement system: θ is the true head motion, θ_T the measured head motion obtained from the measurement device, $\hat{\theta}$ the output of the complementary filter, and $\tilde{\theta}_T$ the error of the measurement device where $\tilde{\theta}$ is the filter's estimation error.

to angular acceleration by using the configuration of the accelerometer pair.

The results of the simulations are shown in Fig. 3. It shows the true θ and the estimate $\hat{\theta}$ of the head orientation, together with the sampled signal θ_T. It can be seen that the error between the true head orientation θ and the estimated one $\hat{\theta}$ diminishes to about 10% of θ. This level of the residual error is comparable to the measurement noise of the HMD measurement system and is adequate for the required image stabilization on the HMD. It also demonstrates that the phase shift between the true θ and the estimated head motion $\hat{\theta}$ is almost eliminated. This is in contrast to the large phase shift between the sampled signal θ_T of the head measurement system and the true head motion θ.

The effect of the finite resolution of the head position and orientation measurement device on the performance of the complementary filter was examined, and it is displayed in Fig. 4. The true head motion was simulated as a low frequency of 0.1 Hz and a small amplitude of the 0.5-deg signal. As a result of the finite resolution of the measurement system, its output is a staircase signal Θ_T, and the error between the two signals is a jagged signal $\tilde{\theta}_T$. The output of the complementary filter, however, is a smooth signal resembling the true head motion although with a slightly larger amplitude. For this case, it should be pointed out that the input of the accelerometer to the filter is zero since the head acceleration is below the threshold of the accelerometer, as mentioned earlier. However, since in this low-frequency range the phase shift due to the sampling process is very low (less than 2 deg), the acceleration input is not essential.

Conclusions

The method based on complementary filtering has been shown to be effective in compensating for the image stabilization error due to sampling delays of helmet-mounted display position and orientation measurements. These delays would have otherwise prevented the stabilization of the image in helmet-mounted displays. In addition, the method has been shown to improve the resolution of the head orientation measurement, especially at low frequencies, hence providing smoother head control commands, which are essential for precise head pointing and teleoperation.

Acknowledgments

This work has been supported in part by the U.S. Air Force Aerospace Medical Research Laboratory, Wright-Patterson Air Force Base, and by the Aerospace Human Factors Research Division, NASA Ames Research Center.

References

[1]Benson, A. J., and Barnes, G. R., "Vision During Angular Oscillation: The Dynamic Interaction of Visual and Vestibular Mechanisms," *Aviation, Space, Environmental Medicine*, Vol. 49, Jan. 1978, pp. 340–345.

[2]Wells, M. J., and Griffin, M. J., "Benefits of Helmet-Mounted Display Image Stabilization Under Whole-Body Vibration," *Aviation, Space, Environmental Medicine*, Vol. 55, Jan. 1984, pp. 13–18.

[3]Wells, M. J., and Griffin, M. J., "Flight Trial of a Helmet-Mounted Display Image Stabilization System," *Aviation, Space, Environmental Medicine*, Vol. 58, April 1987.

[4]Velger, M., and Merhav, S. "Reduction of Biodynamic Interference in Helmet Mounted Sights and Displays," *Proceedings of the 22nd Annual Conference on Manual Control*, Air Force Wright Aeronautical Laboratories, Rept. AFWAL-TR-86-3093, Dayton, OH, Dec. 1986, pp. 139–164.

[5]Merhav, S., "Adaptive Suppression of Biodynamic Interference in Helmet Mounted and Head Down Displays," *Proceedings of the AIAA Guidance, Navigation and Control Conference*, AIAA, Washington, DC, Aug. 1988, pp. 1106–1116.

[6]Raab, F. R., Blood, E. B., Steiner, T. O., and Jones, H. R., "Magnetic Position and Orientation Tracking System," *IEEE Transactions on Aerospace and Electronic Systems*, Vol. AES-15, No. 5, 1979, pp. 709–718.

[7]Higgins, W. T., "A Comparison of Complementary and Kalman Filtering," *IEEE Transactions on Aerospace and Electronic Systems*, Vol. AES-11, No. 3, 1975, pp. 321–325.

True Anomaly Approximation for Elliptical Orbits

Randall D. Peters*
Texas Tech University, Lubbock, Texas 79409

Introduction

THIS Note describes a direct technique for determining true anomaly f on an elliptic orbit at a specified time, without the intermediate step of solving Kepler's equation. The accuracy of the technique is best for small eccentricities e. At $e=0.7$, the maximum error in f is 0.6 degree of arc; for e less than or equal to 0.27, the errors are less than 1 min of arc; and for e less than 0.06, they are smaller than 1 s of arc.

A direct computation of f from mean anomaly M is desirable because fewer computations are necessary, as compared to the usual procedure involving eccentric anomaly E as an intermediate variable. No satisfactory methods to accomplish this are known for large values of e; however, the Fourier-Bessel series[1] is useful for values of e less than about 0.5

$$f = M + \left[2e - (1/4)e^3 + (5/96)e^5\right]\sin M + \left[(5/4)e^2 - (11/24)e^4 + (17/192)e^6\right]\sin 2M + \left[(13/12)e^3 - (43/64)e^5\right]\sin 3M + \left[(103/96)e^4 - (451/480)e^6\right]\sin 4M + (1097/960)e^5\sin 5M + (1223/960)e^6\sin 6M + \mathcal{O}(e^7) \tag{1}$$

It was found that the accuracy of the present algorithm is comparable to that of Eq. (1) to $\mathcal{O}(e^4)$ for small e and is much better than even $\mathcal{O}(e^6)$ for large e.

The present algorithm is important for another reason. It is derived from considerations of elliptic orbit motion as described by the methods of velocity space.[2] Normally, time is not brought naturally into the discussions of these techniques. Usually, the concern is with orbit parameters (such as velocity) at different spatial (rather than time) positions of the orbit. If the time could be brought into the velocity space formalism with elegance that compares to that of the spatial description, than a truly powerful mathematical method would result. The present Note is a first step toward that end.

Velocity Space Foundation

As described by Abelson et al.[2] orbits that are elliptical in terms of displacement vectors become circular in terms of velocity vectors. The center of the velocity circle of invariant radius u is offset by an invariant vector z with respect to the velocity space origin. If one imagines planetary motion about the center of the sun, the vector u is at each moment perpendicular to the planet's position vector r. The magnitude of u is inversely proportional to the planet's angular momentum through the force constant. Additionally, the magnitude of vector z is such that $z = eu$. For the present work, normalization is employed ($u = 1$). There are three points of outstanding significance in the normalized plot. At $f = 0$, the velocity mag-

Received Dec. 26, 1989; revision received May 4, 1990; accepted for publication May 25, 1990.

*Associate Professor of Physics, P.O. Box 4180.